MINERALOGICAL MAGAZINE

VOLUME 40 NUMBER 316 DECEMBER 1976

Crystallization trends of pyroxenes from the alkaline volcanic rocks of Tenerife, Canary Islands

P. W. SCOTT

Department of Geology, the University of Hull, Hull, HU6 7RX

SUMMARY. The alkaline volcanic rocks of Tenerife comprise a compositionally continuous series of ankaramites, alkali basalts, trachybasalts, trachyandesites, trachytes, phonolites, and peralkaline phonolites. Ca-rich pyroxenes occur as phenocrysts throughout the series. They show a limited range of composition from diopside and Ti-rich sahlite in the basic and intermediate rocks, to sodic sahlite in some phonolites. Features of both the sahlite–aegirine and sahlite–hedenbergite trends are present. Sodic ferrosahlites occur as xenocrystal 'green cores' in phenocrysts from some basic and intermediate rocks. The latter are associated with kaersutite xenocrysts and are similar to pyroxenes in some plutonic xenoliths from Tenerife. During the formation of the 'green cores' conditions were more reducing allowing pyroxene compositions to extend through the range sahlite–hedenbergite.

Aegirine-augite and Ti-rich aegirine are present in the groundmass of some phonolites and in pyroclastic boulders of nepheline syenite. The aegirines are associated with magnesioarfvedsonite and aenigmatite, and it is considered that they crystallized under conditions of low oxygen fugacity.

THE alkaline volcanic rocks of Tenerife, Canary Islands, belong to the alkali-basalt–trachyte–phonolite suite characteristic of many Atlantic Islands. They constitute a very undersaturated compositionally continuous series, which is thought to have evolved by protracted crystal fractionation from an alkali basalt parent in a shallow magma chamber (Ridley, 1970; Borley *et al.*, 1971; Borley, 1974). The rocks have been divided into ankaramites, alkali basalts, trachybasalts, trachyandesites, trachytes, and phonolites on a compositional basis, using a plot of the Thornton–Tuttle Differentiation Index against $SiO_2\%$ (Ridley, 1970; Scott, 1970; Borley, 1974). Many of the phonolites are peralkaline, and are often glassy, but coarser-grained pyroclastic blocks, equivalent to the peralkaline phonolites, also occur. These have been referred to as nepheline syenites by Ibarrola and Viramonte (1967). The compositional trends correspond to well-defined petrographic changes, and are summarized in Table I.

Clinopyroxenes are the most abundant ferromagnesian mineral, occurring as a zoned phenocrystal and groundmass phase throughout the suite. Some published data, including a few chemical analyses of pyroxenes from the central Las Canadas area, show a limited range of composition from sahlite or Ca-rich augite to ferrosahlite (Carmichael, 1967; Ridley, 1970). Borley *et al.* (1971) have presented microprobe

© Copyright the Mineralogical Society.

analyses of pyroxenes from some xenoliths that show a similar short compositional range. In the present study further analyses of pyroxenes from the complete volcanic suite have been made, and the compositional range is shown to extend from diopside and Ti-rich sahlite to ferrosahlite and Ti-rich aegirine. Analysis of separate crystals and zones using the electron microprobe has been important in establishing the full trend.

TABLE I. *Summary of petrography of the Tenerife rocks*

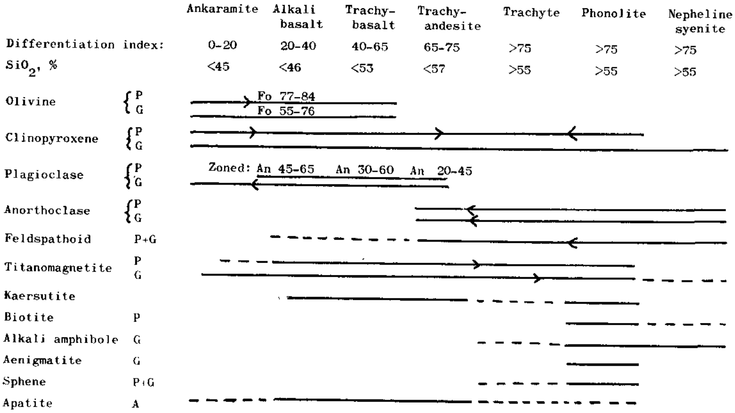

P, phenocrysts;
G, groundmass;
A, accessory.

The position and direction of an arrow refers to a marked decrease in the modal content of the mineral. Discontinuous lines refer to an occasional occurrence.

Except for the ankaramites and nepheline syenites, porphyritic and aphyric varieties are found in each rock type.

Description and optical properties of the pyroxenes. Two main types of pyroxene, sahlite and aegirine, can be recognized. The former occurs as phenocrysts throughout the series, whereas aegirine is restricted to the groundmass of some phonolites and the nepheline syenites.

In the ankaramites, pyroxene phenocrysts are up to 30 mm in diameter and comprise up to 50 % by volume of the rock. The crystals develop the forms {100}, {010}, {110}, and {111} and twins with {100} as twin plane are common. In thin section, the phenocrysts from the ankaramites are pink and pleochroic (α is darker than β or γ) and usually they have a pale pink core, which may have irregular or oscillatory zones. The core is surrounded by a much darker outer zone, which is similar to the groundmass pyroxene. The alkali basalts and trachybasalts have fewer and smaller phenocrysts some of which have a well-developed hourglass structure. Phenocrysts in the trachyandesites are sometimes pale pink but more usually they are a pale watery green. Zoning is less well developed. Most trachytes and phonolites also have small pale watery green phenocrysts and, in these rocks, zoning is uncommon except in crystals that occur in phonolite sheets and dykes cutting the Ancient Series (earliest basement series of lavas described by Fuster *et al.*, 1968). These zoned crystals are subhedral, up to 1·5 mm long and strongly pleochroic (α pale watery green, β pale brownish green, γ pale yellow brown).

Some alkali basalts, trachybasalts, and trachyandesites contain pyroxene phenocrysts with irregular or rounded pleochroic green cores (α medium green, γ pale yellow green) surrounded by a colourless or, more usually, pale pink outer zone.

Rocks in which these 'green cores' occur commonly also contain kaersutite, or a pseudomorph of kaersutite composed of a mass of pyroxenes and opaques. Kaersutite occurs sporadically in all rocks except the ankaramites, and is considered to be present largely as a xenocrystal phase (Scott, 1970).

Aegirine occurs as long prismatic crystals in the fine-grained matrix of some crystalline phonolites. It is strongly pleochroic (α medium green, γ pale yellow green), and forms clusters around nepheline micro-phenocrysts along with pale pink or yellow brown alkali-amphibole, aenigmatite, and opaques. Aegirine in the nepheline syenite occurs as clusters of subhedral to anhedral pleochroic crystals (α bright green, β yellowish green, γ pale yellow-brown) or radiating fibres along with pale brown alkali amphibole, dark brown biotite, sphene, and opaques.

Some optical properties of the pyroxenes are given in Table II. As would be expected from the zoning, measurements cover a wide range of values. There is, however, a general increase in R.I., $2V_\gamma$, and γ:[001] in the phenocrysts towards the phonolites. For crystals with a 'green core', $2V_\gamma$ and γ:[001] are higher in the 'green core' than in the remainder of the crystal. Determination of composition from the optical properties of sahlites (e.g. using curves of Deer, Howie, and Zussman, 1963) gives erroneous values apparently displaced towards hedenbergite. This results from the minor constituents in the sahlites (Na, Ti, Al, and Mn), which have the over-all effect of increasing R.I. and $2V_\gamma$. R.I. measurements on groundmass crystals from the nepheline syenite indicate 75–85 % acmite in the pyroxene (using curves of Deer, Howie, and Zussman, 1963, and Tyler and King, 1967).

TABLE II. *Optical properties of the pyroxenes*

Range of measurements made on the centre of crystals

	β	$2V_\gamma$	γ:[001]
Phenocrysts:			
Ankaramites	1·699–1·711	51–54°	43–50°
Alkali basalts (excluding green cores)	1·703–1·717	51–60	40–58
Alkali basalts: green cores	—	54–65	50–63
Trachybasalts	1·709–1·715	51–3	43–53
Trachyandesites	—	59–63	49–59
Trachytes	—	63–4	—
Phonolites	1·720–1·724	58–71	49–57
Groundmass:			
Phonolites	—	—	α:[001] < 20
Nepheline syenite	α = 1·755–1·765 γ = 1·795–1·805	—	α:[001] < 10

Chemistry of the pyroxenes. Microprobe analysis has shown that most of the pyroxenes are zoned and within a single rock the compositional variation between crystals is often considerable. Some analytical results illustrating the full range of composition are presented in Table III. Complete results, details of experimental conditions, and correction procedures used with the microprobe are given by Scott (1970). Analytical techniques are similar to those described by Borley *et al.* (1971). Unfortunately, groundmass pyroxenes in the phonolite lavas are too fine-grained for analysis, but some determinations were possible of pyroxenes from intrusive phonolites and pyroclastic blocks in which the matrix is somewhat coarser.

TABLE III. *Chemical and microprobe analyses of pyroxenes and alkali amphibole*

No.	1*	2	3	4	5*	6	7	8a	8b	9	10a	10b	11	12	13	14
Spec.	MA15	MA3	MA3	MA19	MA6	24-66	49-66	MA8	MA8	MA8	PS58	PS58	TC38	TC33	PS74	GB8
SiO_2	47.56	51.4	43.8	50.5	47.47	47.8	45.5	46.7	45.4	44.3	43.7	47.0	46.3	43.9	51.2	48.2
TiO_2	2.55	1.3	4.8	1.0	2.14	2.3	2.8	1.0	4.1	4.1	2.0	2.4	3.8	3.3	0.7	1.5
Al_2O_3	5.96	3.2	7.8	4.3	5.52	5.3	7.6	5.7	7.5	8.2	7.2	4.7	6.4	7.6	2.0	3.4
Fe_2O_3	3.40	-	-	-	3.86	-	-	-	-	-	-	-	-	-	-	-
FeO	4.41	4.8	9.1	5.6	3.81	7.5	7.5	16.6	7.4	8.6	12.7	7.9	8.1	8.0	8.3	9.0
MgO	12.61	15.9	11.8	15.3	13.40	13.6	12.4	5.5	12.9	12.1	9.1	14.7	12.6	12.7	12.9	13.1
MnO	0.94	0.1	0.2	0.1	0.69	0.2	0.1	1.1	0.2	0.2	0.4	0.2	0.2	0.1	0.7	0.4
CaO	21.26	23.5	22.4	22.0	21.73	22.2	22.8	20.8	22.9	22.7	22.3	22.8	22.2	23.3	22.0	22.7
Na_2O	0.62	0.3	0.5	0.5	0.79	0.4	0.5	1.8	0.4	0.6	1.4	0.4	0.7	0.6	1.1	0.7
K_2O	0.06	-	-	-	0.00	-	-	0.0	0.0	0.0	-	-	-	-	0.0	0.0
Sum	99.37	100.5	100.4	99.3	99.41	99.3	99.2	99.2	100.8	100.8	98.8	100.1	100.3	99.5	98.9	99.0
Formula on the basis of 6 oxygens:																
Si	1.785	1.89	1.66	1.87	1.781	1.80	1.72	1.84	1.70	1.67	1.71	1.77	1.74	1.67	1.94	1.84
Al^{iv}	0.215	0.11	0.34	0.13	0.219	0.20	0.28	0.16	0.30	0.33	0.29	0.21	0.26	0.33	0.06	0.15
Ti	-	-	-	-	-	-	-	-	--	-	-	0.02	-	-	-	0.01
Al^{vi}	0.049	0.03	0.01	0.06	0.025	0.03	0.06	0.11	0.03	0.04	0.05	-	0.02	0.01	0.03	-
Ti	0.072	0.04	0.14	0.03	0.060	0.07	0.08	0.03	0.12	0.12	0.06	0.05	0.11	0.09	0.02	0.03
Fe^{3+}	0.096	-	-	-	0.109	-	-	-	-	-	-	-	-	-	-	-
Fe^{2+}	0.139	0.15	0.29	0.17	0.120	0.23	0.24	0.55	0.23	0.27	0.42	0.25	0.26	0.26	0.26	0.29
Mg	0.705	0.87	0.67	0.85	0.749	0.76	0.70	0.33	0.72	0.68	0.53	0.82	0.70	0.72	0.73	0.74
Mn	0.024	0.00	0.01	0.00	0.018	0.01	0.00	0.04	0.01	0.01	0.02	0.01	0.01	0.00	0.02	0.01
Ca	0.855	0.92	0.91	0.87	0.873	0.90	0.92	0.88	0.92	0.92	0.94	0.92	0.89	0.95	0.90	0.93
Na	0.045	0.02	0.04	0.03	0.057	0.03	0.04	0.14	0.03	0.05	0.10	0.03	0.05	0.05	0.08	0.05
K	0.003	-	-	-	0.000	-	-	0.00	0.00	0.00	-	-	-	-	0.00	0.00
XY	1.988	2.03	2.07	2.01	2.011	2.03	2.04	2.08	2.06	2.09	2.02	2.08	2.04	2.08	2.04	2.05
Ca	47.0	47.4	48.4	46.0	46.8	47.4	49.5	48.9	48.9	48.9	49.2	46.0	47.8	49.2	47.1	47.2
Mg	38.8	44.9	35.6	45.0	40.1	40.0	37.6	18.3	38.3	36.2	27.7	41.0	37.7	37.3	38.2	37.6
Fe+Mn	14.2	7.7	16.0	9.0	13.1	12.6	12.9	32.8	12.8	14.9	23.1	13.0	14.5	13.5	14.7	15.2
Ac	4.7	2.0	4.1	2.9	5.7	3.0	4.3	15.2	3.2	5.2	10.3	2.8	5.1	7.9	4.8	12.1
Di	73.1	85.3	69.1	83.4	75.2	76.0	74.5	35.9	75.0	70.8	54.6	75.9	72.2	73.5	72.3	71.2
Hd	22.2	12.7	26.8	13.7	19.1	21.0	21.2	48.9	21.8	24.0	35.1	21.3	22.7	21.4	19.8	24.0

Analyses 1 to 24c are clinopyroxenes; 25 is an amphibole. Except for analyses 1, 5, and 24e, total Fe is reported as FeO for sahlites and Fe_2O_3 for aegirines. Geological formations as given by Fuster et al., 1968.

* Chemical analysis. † Calculated on a basis of 23 oxygens. ‡ Ac:Di:Hd ratio obtained by recalculating Fe^{3+}:Mg:(Fe^{2+}+Mn) to 100%.

1. Phenocrysts. Ankaramite. Ancient series, Teno.
2. Core of phenocryst. Ankaramite. Ancient series, Anaga.
3. Groundmass crystal. Ankaramite. Locality as 2.
4. Core of phenocryst. Ankaramite. Ancient Series, Teno.
5. Phenocryst. Alkali basalt. Ancient Series, Anaga.
6. Core pf phenocryst. Alkali basalt. Canadas Series, Portillo escarpment.
7. Core of phenocryst. Alkali basalt. Historic flow, SE. of Las Canadas.

8a and b. 'Green core' and outer zone respectively of crystal from alkali basalt. Ancient Series, Anaga.

9. Groundmass crystal. Alkali basalt. Locality as 8 a and b.

10a and b. 'Green core' and outer zone respec ively of crystal from alkali basalt. Ancient Series, Teno.

11. Microphenocryst. Trachybasalt. Series 3 basalts, Santiago del Teide.
12. Phenocryst. Trachybasalt. Series 3 basalts, W. of Icod.

The main compositional features of the phenocrysts are the over-all high concentration of Ti and Al, limited replacement of Mg by Fe, and the small variation in Na. Cores of phenocrysts from the ankaramites, however, have low Ti and Al (Table III, analyses 2 and 4), but quantities increase in groundmass crystals (analysis 3) and in phenocrysts from the alkali basalts and trachybasalts. Ti and Al decrease and Si increases in phenocrysts and sahlitic groundmass crystals from the trachyandesites, trachytes, and phonolites. Na-rich pyroxenes are restricted to the groundmass of some phonolites (analyses 22–3) and the nepheline syenites (analyses 24a–e): corresponding

TABLE III (*cont.*)

No.	15	16	17	18	19	20	21	22	23	24a	24b	24c	24d	24e	25
Spec.	MA4	MA4	PS27	9-66	PS75	11-66	PS41	PS41	PS84	PS69	PS69	PS69	PS69	PS69	PS84
SiO_2	48.4	47.8	49.1	52.0	52.0	50.3	50.9	51.9	50.8	50.6	50.8	51.3	50.9	50.9	50.9
TiO_2	0.9	1.0	0.9	0.9	0.4	1.0	1.9	1.8	7.2	0.9	1.4	3.6	4.9	2.4	3.1
Al_2O_3	4.2	3.9	3.7	1.6	0.9	2.5	1.8	1.9	0.9	0.8	0.8	1.0	1.2	0.9	2.6
Fe_2O_3	-	-	-	-	-	-	-	28.2	23.6	21.4	24.7	27.1	25.9	20.5	-
FeO	13.5	14.1	12.7	8.6	8.8	12.5	10.3	-	-	-	-	-	-	3.7	12.2
MgO	9.3	8.6	9.5	13.8	12.8	9.0	11.4	1.7	2.1	5.5	3.5	1.8	1.7	3.0	15.1
MnO	1.0	1.1	0.9	0.9	0.9	0.9	1.0	0.5	0.6	1.4	1.2	0.7	0.7	1.0	1.0
CaO	21.4	21.6	20.4	21.7	22.2	21.6	20.0	4.5	3.9	13.3	8.6	3.7	3.6	7.0	5.5
Na_2O	1.6	1.5	1.9	1.4	1.0	1.6	2.5	11.0	11.6	6.2	9.0	12.0	12.0	9.8	6.4
K_2O	-	-	0.0	-	0.0	0.0	0.0	0.0	0.1	0.0	0.0	0.0	0.0	0.0	1.3
Sum	100.1	99.6	99.1	100.9	99.0	99.4	99.8	101.5	100.8	100.1	100.0	101.2	100.9	99.2	98.1
Formula on the basis of 6 oxygens:															
Si	1.86	1.86	1.90	1.94	1.97	1.94	1.93	1.95	1.91	1.93	1.94	1.93	1.92	1.97	7.41†
Al^{iv}	0.14	0.14	0.10	0.06	0.03	0.06	0.07	0.05	0.04	0.04	0.04	0.05	0.05	0.03	0.44
Ti	-	-	-	-	-	-	-	-	0.05	0.03	0.02	0.02	0.03	-	-
Al^{vi}	0.05	0.04	0.07	0.01	0.01	0.05	0.01	0.03	-	-	-	-	-	0.01	-
Ti	0.03	0.03	0.03	0.03	0.01	0.03	0.05	0.05	0.15	-	0.02	0.08	0.10	0.07	0.34
Fe^{3+}	-	-	-	-	-	-	-	0.80	0.67	0.61	0.71	0.77	0.73	0.60	-
Fe^{2+}	0.43	0.46	0.41	0.27	0.28	0.40	0.33	-	-	-	-	-	-	0.12	1.48
Mg	0.53	0.50	0.55	0.76	0.73	0.51	0.64	0.10	0.12	0.31	0.20	0.10	0.10	0.17	3.28
Mn	0.03	0.04	0.03	0.03	0.03	0.03	0.03	0.02	0.02	0.05	0.04	0.02	0.02	0.03	0.12
Ca	0.88	0.90	0.85	0.87	0.90	0.89	0.81	0.18	0.16	0.54	0.35	0.15	0.15	0.29	0.86
Na	0.12	0.12	0.14	0.10	0.07	0.12	0.18	0.80	0.84	0.46	0.67	0.88	0.88	0.73	1.80
K	-	-	0.00	-	0.00	0.00	0.00	0.00	0.00	0.00	0.00	0.00	0.00	0.00	0.40
XY	2.07	2.09	2.08	2.07	2.03	2.03	2.05	1.98	1.96	1.97	1.99	2.00	1.98	2.02	8.28
Ca	47.1	47.4	46.2	45.1	46.4	48.6	44.8	16.4	16.5	35.8	26.9	14.4	15.0	24.0	-
Mg	28.3	26.3	29.9	39.4	37.6	27.9	35.3	9.1	12.4	20.5	15.4	9.6	10.0	14.0	-
Fe+Mn	24.6	26.3	23.9	15.5	16.0	23.5	19.9	74.5	71.1	43.7	57.7	76.0	75.0	62.0	-
Ac	12.1	12.0	14.1	9.4	6.1	12.8	18.0	80	80	44	63	83	82	65.2‡	
Di	53.5	50.0	55.6	71.7	64.1	54.2	64.0	11	15	32	21	11	12	18.5‡	
Hd	34.4	38.0	30.3	18.9	29.8	33.0	18.0	9	5	24	16	6	6	16.3‡	

13. Microphenocryst. Trachyandesite. Recent Salic Series, Mna. Blanca.
14. Phenocryst. Trachyandesite. Recent Salic Series, Las Canadas.
15. Microphenocryst. Trachyte. Ancient Series, Anaga.
16. Groundmass crystal. Trachyte. Locality as 15.
17. Phenocryst. Phonolite. Ancient Series, Anaga.
18. Phenocryst. Crystalline phonolite. Canadas Series, Portillo escarpment.
19. Phenocryst. Glassy phonolite. Recent Salic Series, Mna. Blanca.
20. Groundmass crystal. Phonolite. Canadas Series, El Roque, near San Miguel.
21. Microphenocryst. Phonolite. Canadas Series, Mna. de Guajara.
22. Groundmass aegirine. Phonolite. Locality as 21.
23. Groundmass aegirine. Phonolite. Canadas Series, Tauce escarpment.

24a to d. Matrix aegirine. Nepheline syenite. Pyroclastic boulder, Canadas Series, Las Cañadas.

24e. Matrix aegirine. Nepheline syenite. Average microprobe analysis of 12 crystals, including chemical determination of FeO. Locality as 24 a to d.

25. Magnesioarfvedsonite. Phonolite. Locality as 23. Formula calculated on a basis of 23 oxygens. Total Fe as FeO. Optical data: α pale watery brown, γ pale yellow-brown, 2V 59°, α:[001] 20°.

phenocrysts in the phonolites are Ca-rich. Crystals in the nepheline syenite range in composition from aegirine-augite to aegirine. Many of the aegirines are enriched in Ti, and in the structural formula Na often exceeds total Fe.

The 'green cores' represent a special case of a reversal in zoning. More Fe, Mn, and Na, and less Mg and Ca is present in the 'green core' (analyses 8a and 10a) than in the outer zones (analyses 8b and 10b). Variations in Si, Ti, and Al between core and margin are not always consistent, but the 'green cores' contain relatively more Al for a given Ti content than any other crystal or zone. Hausen (1955) first described these zoned phenocrysts from Tenerife and assumed that the cores were richer in soda: kaersutite was present in the same rocks. Frisch and Schmincke (1969) have found a similar reversal in zoning in xenoliths from Gran Canaria. Green cores within pyroxene phenocrysts from other provinces have been attributed to a chrome-diopside phase (e.g. Huckenholtz, 1966). No Cr has been found in the present samples.

It has been suggested that octahedral Ti and tetrahedral Al in clinopyroxenes from alkali basalt magmas are present as the hypothetical titanium pyroxene $CaTiAl_2O_6$ (Yagi and Onuma, 1967) and a sympathetic relationship of these two ions has been used to indicate substitution of this molecule by replacement for Si and some octahedrally co-ordinated ion (i.e. $M^{2+}_Y + 2Si_Z \rightleftharpoons Ti_Y + 2Al_Z$) (Ross *et al.*, 1970; Barbari *et al.*, 1971; Gibb, 1973). In fig. 1*a* total Al is plotted against Ti in terms of atoms per 6 oxygens. Every determination has been plotted including those of Carmichael (1967), Ridley (1970), and Borley *et al.* (1971). Points are somewhat scattered but over-all trends are evident. There is a general sympathetic relationship between Ti and Al in the sahlites. If substitution is exclusively of the titanium pyroxene, points should cluster along the line of slope 2·0 (i.e. 2Al for each Ti); but there is a general excess of Al for a given Ti content in the sahlites. When Al_Z is plotted against Ti (fig. 1*b*) points cluster nearer the line of slope 2·0 but a small excess of tetrahedral Al remains. This excess of Al_Z along with the octahedral Al is most likely present in the form of Tschermak's molecule (i.e. substitution of the type $M^{2+}_Y + Si_Z \rightleftharpoons Al_Y + Al_Z$ also occurs).

Two further points are illustrated in fig. 1. Firstly, analyses of the 'green cores' and pyroxenes from some xenoliths plot in similar parts of the field and have the highest Al:Ti ratios; this can be taken as indicating an increased amount of Tschermak's molecule. Secondly, some aegirines contain quite large amounts of Ti; Al is approximately constant and insufficient is present to accommodate the Ti in terms of the substitutions discussed above. The range of Ti values is considerable (0·9–7·2 % TiO_2), but the most Na-rich aegirines also contain the largest amount of Ti and, at the same time, contain insufficient Fe^{3+} (as total Fe) to account for all of the Na as acmite, even assuming that Fe^{2+}, and hence the hedenbergite content, is zero. It must be assumed that entry of Na into the pyroxene is balanced by entry of Ti. Flower (1974) has interpreted some of the data of Scott (1970) as indicating a naturally occurring series of aegirines that have substitution of the type $Ti^{4+}_Y + Fe^{3+}_Z \rightleftharpoons Fe^{3+}_Y + Si_Z$ and $Ti^{4+}_Y + Al^{3+}_Z \rightleftharpoons Fe^{3+}_Y + Si_Z$. If all of the Ti can substitute in this way, the amount of this ion in the structural formula should equal the deficiency of Si in the *Z* sites. This is acceptable within experimental error for several of the aegirines, but the most Ti-rich members contain a considerable excess of Ti. Substitution of tetravalent Ti in octahedral sites requires additional substitution of Al or Fe^{3+} for Si, but if part of the Ti is as Ti^{3+}, charge balance would be maintained without additional substitutions. This could explain the excess of Ti but would indicate that crystallization of the aegirines

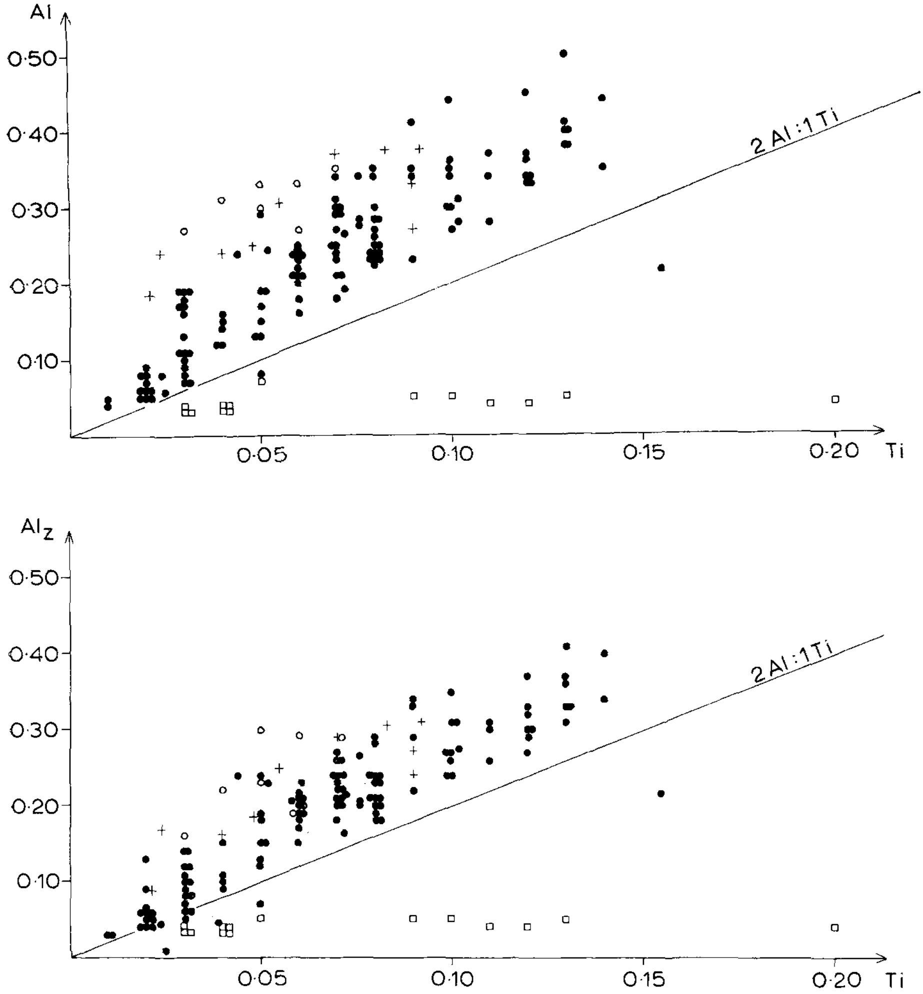

FIG. 1*a*, top: Plot of total Al against Ti calculated on the basis of 6 oxygens. Symbols: ● Sahlites. ☐ Aegirines. ○ 'Green cores'. + Pyroxenes from xenoliths (Borley *et al.*, 1971). *b*, bottom: Plot of Al_Z against Ti calculated on the basis of 6 oxygens. Symbols as in fig. 1*a*.

took place at a considerably lower oxygen fugacity than considered by Flower (1974). A pyroxene containing Na and trivalent Ti has recently been synthesized at high pressure by Prewitt *et al.* (1972).

The sahlites have been expressed in terms of acmite, diopside, and hedenbergite end-members (fig. 2*a*) by allocating Na to form acmite, Mg to form diopside, and total Fe+Mn (less an amount of Fe equal to Na) to form hedenbergite, and recalculating to 100 %. This calculation is not appropriate for the aegirines because of the excess of Na over Fe^{3+}. The amount of acmite is not governed by Na, as is usual, but by Fe^{3+}. As it is not possible to determine ferrous and ferric ions separately with the microprobe, a wet-chemical determination of FeO has been made on a separated pyroxene fraction from the nepheline syenite and included in an averaged microprobe analysis of the aegirine in this rock (analysis 24e). This enables an estimate of acmite: diopside:hedenbergite to be made by recalculating the Fe^{3+}:Mg:Fe^{2+}+Mn ratio to 100 % (point A, fig. 2*a*). Allocation of end-members for the individual aegirine microprobe analyses has been made by partitioning Ca between diopside and hedenbergite: diopside is made from Mg and an equivalent amount of Ca; the remaining Ca is allocated to an equivalent amount of Fe+Mn to make hedenbergite and the remaining Fe is allocated with Na to make acmite. This calculation appears acceptable as, in the averaged analysis, Ca can be partitioned between Mg and Fe^{2+}+Mn to form diopside and hedenbergite respectively with little remainder. Atomic proportions of Ca:Mg:total Fe+Mn recalculated to 100 % are plotted in fig. 3*a*.

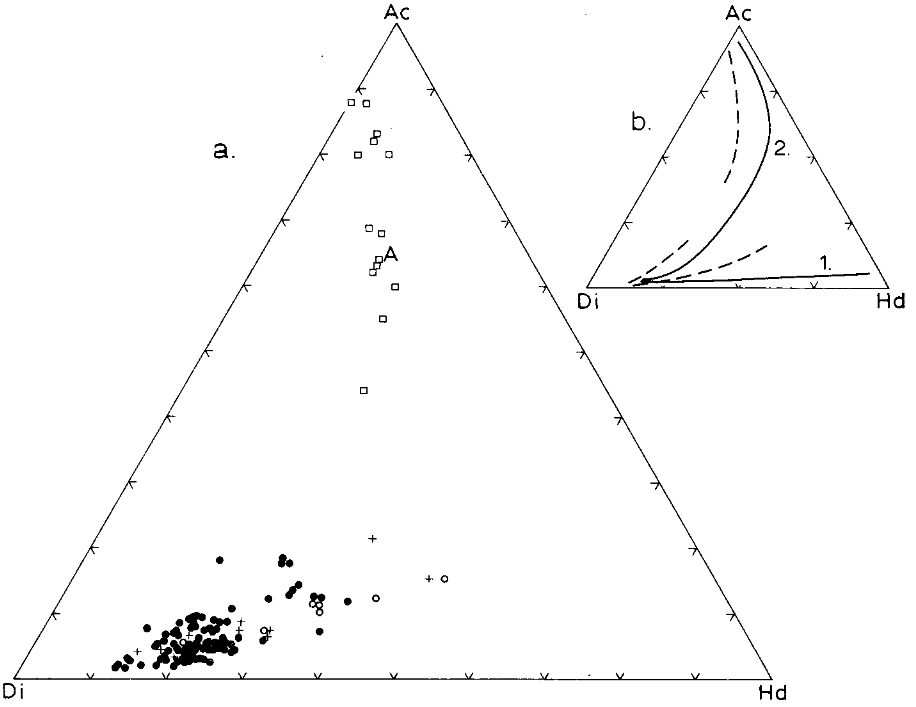

FIG. 2. Compositional variation of the pyroxenes in terms of Ac–Di–Hd end-members. *a*. Symbols as in fig. 1*a*. Point A—see text. *b*. Dashed line—Tenerife trends. Sahlite analyses spread between the two limits. 1. Shiant Isles (Gibb, 1973). 2. Shonkin Sag, Bulk analyses (Nash and Wilkinson, 1970).

Crystallization trends are largely self-explanatory from the diagrams. Within the sahlites there is an over-all limited increase in hedenbergite with some increase in acmite through the sequence from ankaramites to phonolites. Representatives of sahlites from all rock types are present in the region where points are most concentrated. The cores of the phenocrysts from the ankaramites are the most enriched in diopside. The sahlites from the phonolites and trachytes are more variable in composition. Many are enriched in hedenbergite with a small increase in acmite when compared with sahlites from the other rocks. In other phonolites the sahlite is more enriched in acmite with smaller amounts of the hedenbergite molecule. Only the 'green cores' and pyroxenes from some xenolithic material exhibit any strong hedenbergite enrichment. The trend from diopside towards acmite is continued in the aegirines. The aegirines from the nepheline syenite show a considerable spread of values (44–88 % acmite). The averaged analysis using the chemical determination of FeO falls in the middle of the range (point A). Points of similarity exist with crystallization trends from both the Shonkin Sag laccolith (Nash and Wilkinson, 1970) and the Shiant Isles sill (Gibb, 1973) (figs. 2*b* and 3*b*), although the aegirines are rather more diopsidic than those from Shonkin Sag and extreme Fe-enrichment towards a sodic hedenbergite as in the Shiant Isles does not occur in the 'green cores'. The sahlites cluster nearer to the 50 % Ca line (fig. 3) than pyroxenes from the Shiant Isles. Gibb (1973) states that this is typical of pyroxenes crystallizing from strongly under-saturated magmas. Pyroxene compositions just below and above the 50 % Ca line reflect

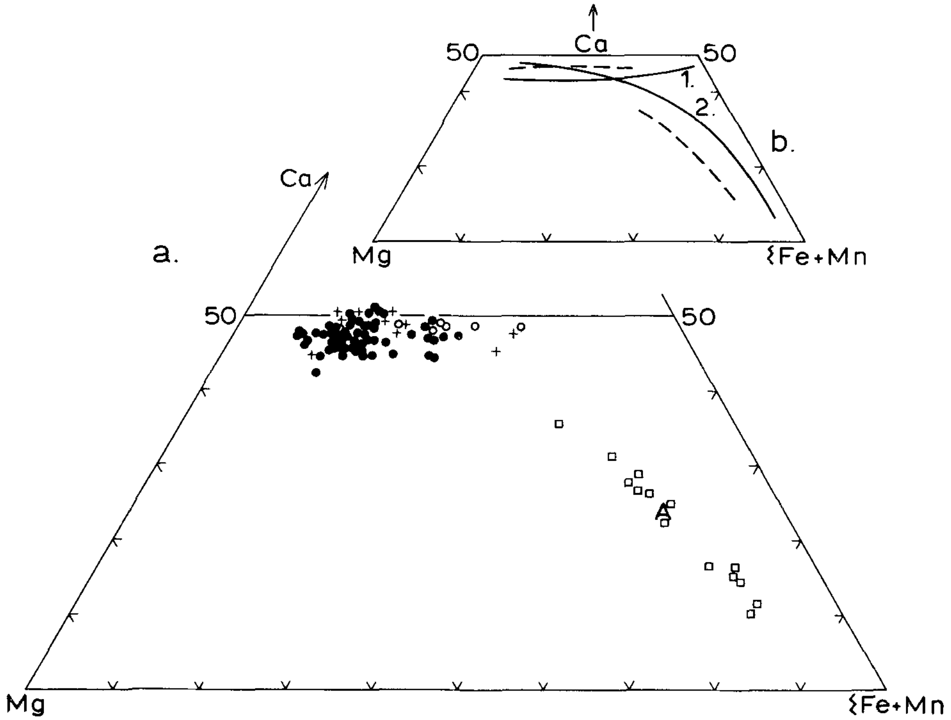

FIG. 3. Compositional variation of the pyroxenes in terms of Ca : Mg : ΣFe + Mn ratio. *a*. Symbols as in fig. 1*a*. *b*. Dashed line—Tenerife trends. 1. Shiant Isles (Gibb, 1973). 2. Shonkin Sag, Soda syenite (Nash and Wilkinson, 1970).

the increased substitution of $CaTiAl_2O_6$. The trend towards the Fe corner in fig. 3 represents the entry of Na and Fe^{3+} in the aegirines instead of Ca and Fe^{2+}.

Discussion

Ridley (1970) concluded that the parental magma for Tenerife and probably other Canary Islands is of alkali basalt composition. Pyroxene is considered to have been the first phase to have crystallized followed by olivine and titanomagnetite, and then plagioclase at a later stage. Accumulation of pyroxene and olivine has led to the development of the ankaramites, and pyroxenite and dunite xenoliths. At depth cumulate rocks might be expected, such as wehrlites, which appear on the adjacent island of Gomera. The composition of the first pyroxene, which will be similar to that in the cores of the ankaramite phenocrysts and pyroxenite xenoliths (Borley *et al.*, 1971, analysis P1), differs somewhat from that which crystallized at a later stage. It is more diopsidic and contains lesser amounts of $CaTiAl_2O_6$. The latter may reflect crystallization at greater depths, as Yagi and Onuma (1967) have shown that the solubility of $CaTiAl_2O_6$ in diopside decreases with increase in pressure above 10 kb. Crystallization of pyroxene at a lower pressure in phenocrysts from the alkali basalts, trachybasalts, and trachyandesites seems to enable more $CaTiAl_2O_6$ to be accommodated in the pyroxene, even though at this stage titanomagnetite is an accompanying liquidus phase. Groundmass crystals in the basic rocks forming at surface pressures contain the greatest amounts of Ti and Al.

The change in composition of pyroxene crystallizing from successively differentiated alkali basaltic magmas may be towards extreme enrichment in hedenbergite or, after some small increase in hedenbergite, towards acmite. The controlling factor has been considered to be the oxygen fugacity of the magma, high or increasing f_{O_2} favouring the oxidation of iron and hence solid solution of acmite (Aoki, 1964; Yagi, 1966). The crystallization trend towards acmite in the phonolites could be taken as indicating a high f_{O_2} during later stages of differentiation. At high f_{O_2} the iron will be present largely as Fe^{3+} and, providing the liquid has built up a sufficient concentration of Na, aegirine can then form. This is most likely restricted to the peralkaline phonolites, in others the groundmass pyroxene being a sodic sahlite. All phenocrystal pyroxenes in the phonolites are also sahlitic. Bailey (1969) has stated that at low pressure acmite melts at temperatures below that of other major components in phonolites. Thus aegirine is unlikely to have crystallized as a phenocryst in the magma chamber.

Crystallization under conditions of high f_{O_2} cannot explain the trend shown by the 'green cores' and some xenolith pyroxenes towards enrichment in hedenbergite. Also the spread in composition of phenocrysts from the phonolites showing features of both hedenbergite and acmite enrichment indicates that a more delicate balance between the two trends may exist. In recent years crystallization of some pyroxenes belonging to the sahlite–hedenbergite and sahlite–aegirine trends has been interpreted as developing with falling f_{O_2} (Nash and Wilkinson, 1970; Gibb, 1973) (figs. 2*b* and 3*b*). As crystallization occurs the temperature and f_{O_2} fall, but at a rate less than that required to maintain a constant $Fe^{2+}:Fe^{3+}$ ratio in the liquid and the activity of

Fe^{3+} increases. The difference between the two trends is caused by a different rate of fall of f_{O_2} with temperature, the slower rate of fall of f_{O_2} promoting the sahlite–aegirine trend (Gibb, 1973). The crystallization trends of the Tenerife pyroxenes may be related in a similar way to falling f_{O_2}, but conditions in the magma chamber during crystallization of the phenocrysts may change, causing differences in the $Fe^{2+}:Fe^{3+}$ ratio and hence altering the composition of the pyroxene. The mechanism whereby the changes could occur is likely to be complex and could be controlled by many factors including the effect of build-up of P_{H_2O} and other volatiles in the magma chamber between eruptions.

It is considered that the similar chemistry of the 'green cores' and some xenolith pyroxenes indicates a genetic connection, and this is further substantiated when it is remembered that both are associated with kaersutite. Most likely the 'green cores' are xenocrysts that have been mantled by the more normal pyroxene, and they formed at the same stage of crystal fractionation as the kaersutite. The kaersutite megacrysts and xenocrysts, and kaersutite-bearing xenoliths are thought to form by separation in the magma chamber from liquids of intermediate composition (Scott, 1970; Borley *et al.*, 1971; Borley, 1974). Conditions during formation of the kaersutite and 'green cores' must have been more reducing (i.e. the rate of fall of f_{O_2} with temperature promotes the sahlite–hedenbergite trend) in contrast to the environment during crystallization of phenocrystal pyroxenes from the intermediate and phonolitic magmas. The reversal in zoning in pyroxenes associated with kaersutite has also been examined by Frisch and Schmincke (1969) in inclusions from Gran Canaria. They similarly explain the reversal in terms of changes in f_{O_2}.

Finally, conditions of crystallization of the groundmass aegirine in the phonolites and nepheline syenites must be considered. Bailey (1969) has found that acmite crystallizes from a hydrous synthetic melt under oxygen fugacities as low as those defined by the fayalite–magnetite–quartz buffer, and work on the Shonkin Sag laccolith (Nash and Wilkinson, 1970) has shown that acmitic pyroxenes can crystallize at low oxygen fugacities, but require fugacities greater than those for which the assemblage fayalite plus magnetite is stable. The latter assemblage is normally associated with a sodic hedenbergite and not acmite (e.g. pantellerites, Carmichael, 1962). In the Shonkin Sag laccolith the Na-rich pyroxene is associated with arfvedsonite, and, in the present peralkaline phonolites and nepheline syenites, aegirine is associated with alkali amphibole and on occasions aenigmatite. Both are very fine-grained, but determination of optical properties and one analysis of the amphibole have been possible (Table III, analysis 25). The amphibole is a magnesioarfvedsonite, and is similar to others described by Sutherland (1969) from fenites. Bailey (1969) deduced that an arfvedsonitic amphibole can only be stable in peralkaline liquids under low fugacities of oxygen, but that the assemblage acmite–arfvedsonite may indicate a slightly higher f_{O_2} or a lower degree of peralkalinity in the magma. The presence of aenigmatite is also a reflection of crystallization under relatively low f_{O_2}. Synthetic aenigmatites in experiments of Ernst (1962) formed only with very low fugacities controlled by the magnetite–wüstite and wüstite–iron buffers and low fluid pressure, but more recently experiments of Lindsley (1970) have extended the stability field as far as the fayalite–magnetite–quartz buffer. It must therefore be concluded that f_{O_2} was low during crystallization of the Tenerife phonolites and nepheline syenites, but where aenigmatite is absent a slight increase may be possible. This conclusion is at variance with that made by Flower (1974) who considered that the substitution of Ti in aegirine indicates extremely high f_{O_2}. However, the observed chemistry of the aegirines may be best explained by assuming that some of the Ti is in the trivalent state and thus lower f_{O_2} conditions would operate.

Acknowledgements. The experimental part of this work was carried out under the encouragement and supervision of Dr. G. D. Borley at Imperial College, London during the tenure of a N.E.R.C. Research Studentship. I am grateful to Mr. P. Suddaby for instruction on microprobe techniques, and to Dr. J. Nolan for valuable discussion. I thank Drs. G. D. Borley and N. S. Angus for critically reading the manuscript.

REFERENCES

AOKI (K.), 1964. *Amer. Min.* **49**, 1199–1223.
BAILEY (D. K.), 1969. *Amer. Journ. Sci.* (*Schairer Vol.*) **267A**, 1–16.
BARBARI (F.), BIZOUARD (H.), and VARET (J.), 1971. *Contr. Min. Petr.* **33**, 93–107.
BORLEY (G. D.), 1974. *Proc. Geol. Ass.* **85**, 259–79.
—— SUDDABY (P.), and SCOTT (P. W.), 1971. *Contr. Min. Petr.* **31**, 102–14.
CARMICHAEL (I. S. E.), 1962. *Min. Mag.* **33**, 86–113.
—— 1967. *Contr. Min. Petr.* **18**, 175–98.
DEER (W. A.), HOWIE (R. A.), and ZUSSMAN (J.), 1963. *Rock Forming Minerals.* **2.** *Chain Silicates.* Longmans, London.
ERNST (W. G.), 1962. *Journ. Geol.* **70**, 689–736.
FLOWER (M. F. J.), 1974. *Amer. Min.* **59**, 536–48.
FRISCH (T.) and SCHMINCKE (H. U.), 1969. *Bull. Volcanologique*, **33**, 1073–88.
FUSTER (J. M.), ARANA (V.), BRANDLE (J. L.), NAVARRO (M.), ALONSO (U.), and APARICIO (A.), 1968. *Geologia y Volcanologia de las Islas Canarias: Tenerife.* Instituto 'Lucas Mallada', Madrid.
GIBB (F. G. F.), 1973. *Journ. Petrology*, **14**, 203–30.
HAUSEN (H.), 1955. *Soc. Sci. Fennica. Comment. Physico-Mathematicae*, **18**, (1), 1–254.
HUCKENHOLTZ (H. G.), 1966. *Contr. Min. Petr.* **12**, 73–95.
IBARROLA (E.) and VIRAMONTE (J.), 1967. *Estud. Geol.* **23**, 215–22.
LINDSLEY (D. H.), 1970. *Carnegie Inst. Wash. Year Book* **69**, 188–90.
NASH (W. P.) and WILKINSON (J. F. G.), 1970. *Contr. Min. Petr.* **25**, 241–69.
PREWITT (C. T.), SHANNON (R. D.), and WHITE (W. B.), 1972. Ibid. **35**, 77–82.
RIDLEY (W. I.), 1970. Ibid. **26**, 124–60.
ROSS (M.), BENCE (A. E.), DWORNIK (E. J.), CLARK (J. R.), and PAPIKE (J. J.), 1970. *Science*, **167**, 628–30.
SCOTT (P. W.), 1970. *Ferromagnesian Minerals from the Volcanic Suite of Tenerife, Canary Islands.* Unpublished Ph.D. thesis, University of London.
SUTHERLAND (D. S.), 1969. *Contr. Min. Petr.* **24**, 114–35.
TYLER (R. C.) and KING (B. C.), 1967. *Min. Mag.* **36**, 5–21.
YAGI (K.), 1966. *Amer. Min.* **51**, 976–1000.
—— and ONUMA (K.), 1967. *Journ. Fac. Sci. Hokkaido Univ. Ser. IV*, **13**, 463–83.

[*Manuscript received 3 July 1975, revised 30 January 1976*]

Errata: Table III. Al_2O_3 in anal. 5 is 5·22; and Ac in anals. 12, 13, 14 is 5·1, 7·9, 4·8 respectively. In the key, no. 6, *for* pf *read* of, and *for* respec ively *read* respectively.